

See discussions, stats, and author profiles for this publication at: <https://www.researchgate.net/publication/234035656>

Alignment of Liquid Crystal on Poly[methyl(phenyl)silylene] Films Treated with Polarized UV Light

ARTICLE *in* MACROMOLECULES · JANUARY 2006

Impact Factor: 5.8 · DOI: 10.1021/ma050278h

CITATIONS

12

READS

18

6 AUTHORS, INCLUDING:



[Yuriy Zakrevskyy](#)

Cologne University of Applied Sciences

32 PUBLICATIONS 484 CITATIONS

SEE PROFILE



[Andrey Kadashchuk](#)

Institute of Physics of the National Academy ...

104 PUBLICATIONS 1,344 CITATIONS

SEE PROFILE

Alignment of Liquid Crystal on Poly[methyl(phenyl)silylene] Films Treated with Polarized UV Light

Stanislav Nešpùrek*

Institute of Macromolecular Chemistry, Academy of Sciences of the Czech Republic, Heyrovsky Sq. 2, 162 06 Prague 6, Czech Republic, and Chemical Faculty, Technical University of Brno, Purkynova 118, 612 00 Brno, Czech Republic

Yuriy Zakrevskyy, Joachim Stumpe, and Beate Sapich

Fraunhofer Institute for Applied Polymer Research, Science Campus Golm, Geiselbergstr. 69, D-14476 Potsdam, Germany

Andrey Kadashchuk

Institute of Physics, National Academy of Sciences of Ukraine, Prospekt Nauki 46, 252650 Kiev 22, Ukraine

Received February 8, 2005; Revised Manuscript Received November 1, 2005

ABSTRACT: The alignment of liquid crystal (LC) on poly[methyl(phenyl)silylene] (PMPSi) films treated with linearly polarized light is reported. Simultaneous measurements of the photoinduction of dichroism in the PMPSi films and of the azimuthal anchoring energy of LC on these films revealed the absence of a correlation in the kinetics of both processes. The azimuthal anchoring energy of LC reaches its maximum at the beginning of the irradiation where the dichroism is still neglectful. On further irradiation the dichroism increases, but the azimuthal anchoring energy of the LC drops to zero. To explain this behavior, detailed investigations of photoinduced processes in PMPSi films caused by irradiation with UV light were performed. It was found that anisotropic distribution of ion pairs in the direction of the polarization of the exciting light plays an essential role in the alignment of LC.

Introduction

Photopolymers are believed to allow the development of a “clean” noncontact method of the LC alignment important for the display operation, which permits control of the direction of the easy axis of orientation and the anchoring energy of LC over an aligning surface.¹ Polysilanes with their uninterrupted chains of silicon atoms and with significant electron delocalization along the polymer chain² are a new class of photosensitive polymers with unusual properties. They also possess promising photoconductive properties.^{3–7} Upon UV irradiation at room temperature they undergo complex photodegradation processes, like photochemical cleavage of Si–Si bonds, oxidation to polysiloxanes, cross-linking, photoablation, formation of quasi-stable electron–hole pairs, and metastable electronic states. For these reasons, polysilanes have been studied as photoresists.^{2,8} It is expected that interfacial properties of polysilanes are also modified by these processes, too. From the technological point of view, polysilanes are materials soluble in many organic solvents, i.e., easy processable by conventional techniques like spin-coating and casting. This property together with the above-mentioned photoprocesses makes it possible to use polysilanes as substrates enabling the alignment of LCs⁹ and fabrication of polarized light-emitting diodes.¹⁰ In this paper the phenomenon consisting of the angular-dependent photoinduced cleavage of Si–Si bond and formation of ion pairs and in the formation of other photoproducts preferentially within segments oriented along light polarization, allowing liquid crystalline photoalignment, is described in detail. As a model material poly[methyl(phenyl)silylene] is used.

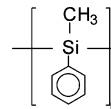


Figure 1. Chemical structure of poly[methyl(phenyl)silylene] (PMPSi).

Experimental Section

Synthesis of Poly[methyl(phenyl)silylene] (PMPSi). The chemical structure of poly[methyl(phenyl)silylene] is shown in Figure 1.

The polymer was prepared by the Wurtz synthesis from corresponding dichlorosilane, which was freshly distilled prior to use. The monomers were reacted with sodium dispersion in boiling toluene.

15 g (0.65 mol) of oxide-free sodium was dispersed in 200 mL of boiling toluene under argon. To increase the yield, 2 mL of diglyme was added to some batches. 50 mL (0.26 mol) of freshly distilled dichloro(methyl)phenylsilane in 50 mL of toluene was dropped into the dispersion until the color of the reaction mixture changed to blue, indicating the start of the reaction. The blue color is explained by defects in the formed NaCl lattice or by sodium colloids. The rest of the monomer solution was added dropwise in the dark in the course of 1 h. After 2 h at 140 °C, the reaction was quenched at room temperature by addition of 2 mL of a butyllithium solution (butyllithium reacted with end chlorine atoms of polymer chains and terminated consecutive reactions and cross-linking). The residual sodium was reacted, under ice cooling, first with 100 mL of ethanol and then with 100 mL of H₂O. After separation of layers, the organic phase was washed three times with 50 mL of H₂O and then dried with anhydrous magnesium sulfate. Cross-linked and insoluble portions were separated by centrifugation with a Beckmann ultracentrifuge J21C at 14 000 rpm for 30 min. The polymer was then precipitated by addition of 600 mL of isopropyl alcohol. For purification, it was twice reprecipitated from a THF solution with isopropyl alcohol. The low-molecular-weight portion was

* To whom correspondence should be addressed: Tel +420-222-514-610; Fax +420-222-516-969; e-mail nespurek@imc.cas.cz.

separated by 1 h extraction with boiling ether. The polymer was dissolved in THF once again, the solution was centrifuged and the polymer reprecipitated twice from THF with isopropyl alcohol. The polymer was then dried at 13 mbar for 48 h. The yield was 34% (47% when diglyme was used). The polymer possessed a unimodal but broad molar mass distribution ($M_w = 4 \times 10^4 \text{ g mol}^{-1}$, $M_w/M_n = 2.7$; SEC averages relative to polystyrene standards). Molar mass was determined using GPC (Laboratory Instruments, Czech Republic). Before deposition of films, the polymer was three times reprecipitated from a toluene solution with methanol. The final toluene solution was centrifuged (12 000 rpm, 15 min).

Sample Preparation and Measurements. Thin films (thickness 0.1–0.5 μm) were prepared by casting or spin-coating (2000 rpm) of toluene solution on silica glass substrates. After deposition, the films were kept in air for 24 h at room temperature and then dried at 0.1 Pa and 330 K for at least 4 h.

Irradiation of films for the induction of dichroism and liquid crystal alignment experiments was performed with linearly polarized light of He–Cd laser ($\lambda = 325 \text{ nm}$). Light intensity at the sample position was 0.2 and 10 mW cm^{-2} . The UV–vis polarized spectral measurements were carried out with a dispersive double-beam spectrometer (Perkin-Elmer, Lambda 19) equipped with a Glan-Thomson prism mounted on computer-driven stepping motor.

To estimate azimuthal anchoring energy of LC on irradiated PMPSi films, a twist angle in a combined cell (LC cell in which one substrate was covered with photopolymer (PMPSi) and the other one with a rubbed polyimide layer) was measured. The angle between the easy axis of LC orientation on PMPSi layer and the rubbing direction on polyimide was fixed to $\alpha = 45^\circ$. The twist angle φ of LC was measured using a polarizing microscope. The azimuthal anchoring energy W was calculated from the formula¹¹ $2\varphi + \xi \sin 2(\varphi - \alpha) = 0$, where ξ is the anchoring parameter, $\xi = Wd/K_{22}$, K_{22} is the twist elastic constant of LC, and d is the thickness of the cell. For these measurements the cells with thickness 20 and 50 μm were constructed and filled with LC ZLI-4801-000 (Merck) in the isotropic phase (100 $^\circ\text{C}$, clearing point 90 $^\circ\text{C}$) and then slowly cooled to room temperature. To estimate the order of anchoring energy, we used $K_{22} = 6.5 \text{ pN}$ as value for the twist elastic constant.

Thermostimulated luminescence (TSL) measurements were performed in the fractional heating regime, which allowed to determine the trap depth and frequency factor.¹² After cooling, PMPSi samples (thickness ca. 3 μm) were irradiated with UV light (a high-pressure 500 W mercury lamp with optical filters).

Flash photolysis was measured on films using the irradiation of single 20 ns flashes ($\lambda_{\text{inc}} = 325 \text{ nm}$) emitted from a ruby laser that was operated in conjunction with a frequency doubler. Photodegradation experiments were carried out using a mercury discharge lamp. The wavelength of incident light ($340 \pm 20 \text{ nm}$) was selected using a filter.

Results and Discussion

Photoinduced Dichroism and Liquid Crystal Alignment. Poly[methyl(phenyl)silylene] chain, with methyl and phenyl groups on each silicon atom, behaves as one-dimensional system with weak intermolecular interactions. The molecular feature of the material is reflected in the energy diagram of electronic states. It has been shown¹³ that the first longest-wavelength absorption band with the maximum at $\lambda_{\text{max}} = 325 \text{ nm}$ (absorption coefficient $\alpha = 7.6 \times 10^4 \text{ cm}^{-1}$) is formed mainly by the delocalized $\sigma-\sigma^*$ transitions in the Si backbone. The dipole moment of this transition is directed along the polymer backbone. The $\pi-\pi^*$ aryl-like excitations are responsible for the short wavelength absorption with the maximum at 276 nm ($\alpha = 5.2 \times 10^4 \text{ cm}^{-1}$).

Irradiation of the PMPSi film with linearly polarized light of He–Cd laser ($\lambda_{\text{max}} = 325 \text{ nm}$) under ambient conditions produced photoinduced changes in the UV spectra of the film. The changes were found to be independent of the power density

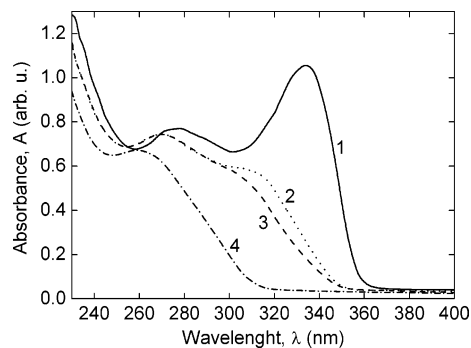


Figure 2. Changes in polarized UV spectra of PMPSi film on irradiation with linearly polarized light of He–Cd laser ($\lambda = 325 \text{ nm}$, $P = 10 \text{ mW cm}^{-2}$): (1) spectrum of as-prepared film; (2) spectrum parallel to the polarization of the exciting light after the exposure dose 0.2 J cm^{-2} ; (3) spectrum perpendicular to the polarization of the exciting light after the exposure dose 0.2 J cm^{-2} ; (4) spectrum measured after the exposure dose 12.0 J cm^{-2} .

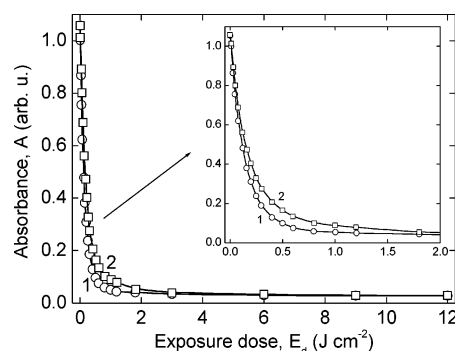


Figure 3. Changes of absorbance of PMPSi film at 333 nm on irradiation with linearly polarized light of He–Cd laser ($\lambda = 325 \text{ nm}$, $P = 10 \text{ mW cm}^{-2}$): (1) parallel to the polarization of the exciting light; (2) perpendicular to the polarization of the exciting light. Inset: details for low-exposure doses.

of the exciting light but dependent on the exposure dose. These changes are presented in Figure 2. The photoinduced changes were found to be angular dependent with respect to the polarization of the actinic light.

The long-wavelength absorption band is caused by the all-trans main-chain segments separated by gauche conformations (see the results in the following section). Thus, a polysilane film is an assembly of energetically different, weakly coupled Si–Si chain segments. The exposure with the linearly polarized light results in the angular dependent excitation of the main chain segments, which are oriented parallel to the electric field vector of the exciting light.

The change in absorbance at 333 nm is presented in Figure 3. The decrease in the absorbance was not very sensitive to light polarization. The absorbance parallel and perpendicular to the polarization of the actinic light decrease almost simultaneously. From the changes in absorbance at this wavelength the appropriate change of the dichroism $D = (A_{\text{max}} - A_{\text{min}})/(A_{\text{max}} + A_{\text{min}})$ was calculated (Figure 4). Initially, the dichroism increases with the conversion of PMPSi when long all-trans chain segments absorb. The dichroism reaches the maximum value ca. 0.27 at the exposure dose of about 1 J cm^{-2} when the vast majority of chain segments are photodegraded (the absorbance is less than 10% of the initial value), and on subsequent irradiation it practically goes to zero. The dichroism is related to the remaining, still intact chain segments perpendicular to the electric field vector of the incident light.

The polysilane segments oriented parallel to the electric field vector undergo photoinduced scission of the Si–Si backbones

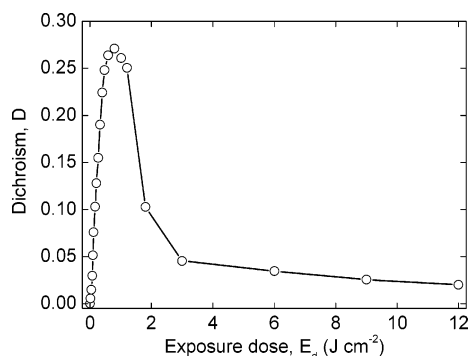


Figure 4. Changes of dichroism calculated at 333 nm on irradiation of PMPSi film with linearly polarized light of He–Cd laser ($\lambda = 325$ nm, $P = 10$ mW cm $^{-2}$).

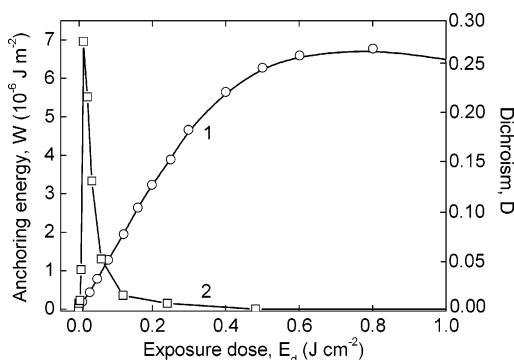


Figure 5. Changes of dichroism calculated at 333 nm (1) and azimuthal anchoring energy of liquid crystal (2) on irradiation of PMPSi film with linearly polarized light of He–Cd laser ($\lambda = 325$ nm, $P = 10$ mW cm $^{-2}$).

(quantum yield for films is 0.016 bond scission per photon). The photodegradation results in a decrease in molar mass of the polymer with the irradiation dose and in the shift of the absorbance maximum to shorter wavelengths (Figure 2). In the photodegradation, polysiloxanes and polymer networks are also formed. So far, the anisotropy of the formation of these products has not been measured, and their contribution to the LC alignment is not clear yet. The fact that LC alignment was not influenced by washing the polymer surface with ethanol, which should remove the polysiloxanes, suggests that this species are not very important in the alignment process.

To measure the azimuthal anchoring energy of the liquid crystal on the polymer surface PMPSi films were irradiated with different exposure doses through a mask. The cells were filled with the liquid crystal (for details see the Experimental Section). The azimuthal anchoring energy was calculated from the twist angle of the liquid crystal in the cell measured by polarizing microscope. The easy axis of the LC alignment was induced parallel to the polarization of the actinic light. PMPSi produced a good quality of planar alignment with zero pretilt, which was thermostable up to 100 °C and did not show any fatigue at least for several months. The dependence of azimuthal anchoring energy W on the exposure dose is shown in Figure 5. The dependence of the anchoring energy on the exposure showed a rather sharp maximum (dose ca. 0.025 J cm $^{-2}$). The maximum value of $W = 7.0 \times 10^{-6}$ J cm $^{-2}$ agrees with the value obtained by other authors.¹⁴

If one compares the shapes of the curves of dichroism and azimuthal anchoring energy, it is easily to notice that they look qualitatively similar (cf. Figures 4 and 5). The only difference is that the direction of preferential orientation of remaining (nonphotodegraded segments) of the chains and the observed direction of the easy axis of the liquid crystal alignment are

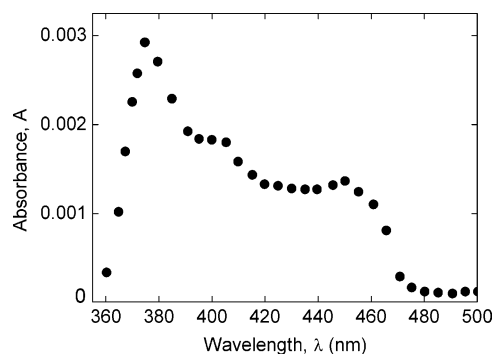


Figure 6. Flash photolysis transient optical absorption spectrum of thin rigid PMPSi film.

orthogonal. To explain this experimental fact, it was proposed by us¹⁵ that irradiation with UV light results in the formation of ion pairs with a long lifetime, which are stable even at room temperature. This idea was used later by Yaroshchuk et al.¹⁴

Simultaneous measurement of dichroism and azimuthal anchoring energy reveals that the azimuthal anchoring energy reaches its maximum just at the beginning of the irradiation where the dichroism is still negligible. On further irradiation the dichroism increases, but the azimuthal anchoring energy of the liquid crystal drops to zero. These results are presented in Figure 5. To explain this behavior, we will first discuss the photoprocesses which are induced by irradiation of PMPSi with UV light.

Photoinduced Processes. The irradiation of PMPSi film at $\lambda_{\text{inc}} = 347$ nm causes a transient absorption¹⁶ with strong maxima around 460 and 370 nm as it follows from Figure 6. These peaks are attributed to silylene radicals and to localized (i.e., terminal) silyl radicals and/or delocalized cation radicals,^{17–20} respectively (II and III in Figure 7). It follows from kinetic studies that the lifetimes of these radicals are about 4 and 260 μ s, respectively, but long-lived species exist depending on the morphology distribution of polymer chains. The kinetics of the radicals suggest that they can recombine, but a photoinduced Si–Si bond scission can also occur. An irradiation in air can cause the formation of siloxane species (IV in Figure 7) as it follows from the IR spectrum where additional peaks at 1122 and 1111 cm $^{-1}$ were found.²¹ During these $\sigma \rightarrow \sigma^*$ excitations (I, Figure 7), i.e., the excitations of Si–Si bonding electrons, the electron is promoted from the bonding to an antibonding orbital. This process can be followed by electron transfer on the polymer chain (V, Figure 7). Thus, an electron–hole pair is formed. However, the pairs generated in the same chain segment very often recombine geminately with a very fast decay rate, due to the electron delocalization in the Si backbone. An interchain or intrachain (VI, Figure 7) electron transfer to phenyl moieties is necessary for the stabilization of the charge transfer state. A similar situation exists during the $\pi \rightarrow \pi^*$ transition, i.e., the phenyl group excitations, when a Frenkel exciton is formed. A positive hole from the excited phenyl group is transferred to the Si–Si main chain, and a positive main chain polaron is formed. For both the types of excitations, the intrachain electron transfer from the main Si chain to phenyl group is quite probable²² because the ground state is predominantly $\sigma_{\text{Si–Si}}$, i.e., ionization potential $I_p(\text{Si–Si}) < I_p(\text{benzene})$. The photoelectron spectral band of benzene was found at 9.24 eV (π , e_{1g})²³ and of hexamethyldisilane at 8.69 eV ($\sigma_{\text{Si–Si}}$).²⁴ The Si–Si grouping is unique in the sense that I_p of the ($\sigma_{\text{Si–Si}}$) electrons is lower than that of the benzene π -electrons. The electron transfer to benzene ring is also in agreement with reduction experiments.²⁵ The case of reduction obeys the order $(\text{Me}_2\text{Si})_5 > \text{C}_6\text{H}_6 > (\text{Me}_2\text{Si})_6 > \text{Me}(\text{Me}_2\text{Si})_n\text{Me}$, where Me is methyl. In

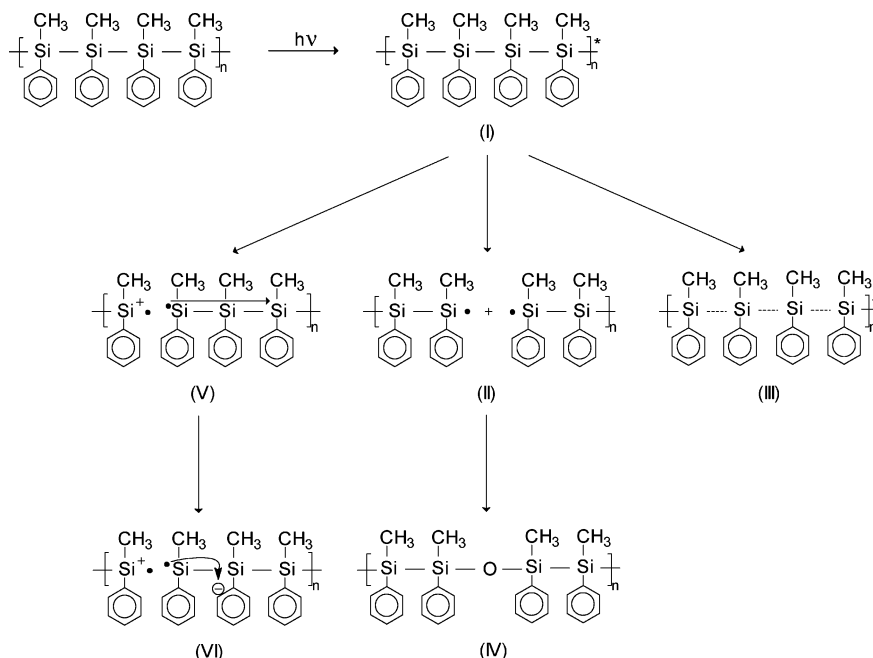


Figure 7. Formation of photospecies during the (σ - σ^*) excitation of PMPSi.

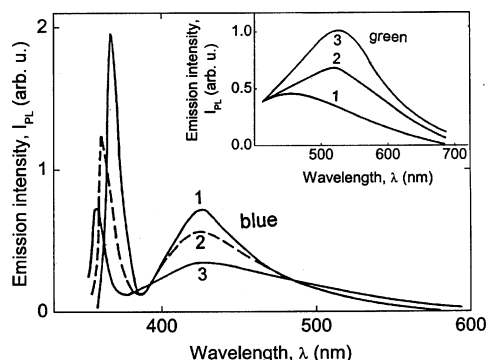


Figure 8. Low-temperature photoluminescence spectra of PMPSi film without (curve 1) and with 366 nm "photodegradation exposure" at room temperature (curve 2–5 min, curve 3–200 min). Inset: defect (weakened bond) photoluminescence emission spectra ($\lambda_{\text{exc}} = 333$ nm).

this way the charge transfer (σ , π^*) excitons and more stable ion pairs are formed. In the external electric field the ion pairs can dissociate, and free charge carriers (polarons) are generated.

During the photodegradation with UV light some changes in the absorption spectrum were detected (Figure 3). The intensity of the long wavelength band, which arises from the delocalized σ - σ^* electronic transitions, decreased with the level of the photodegradation, and its maximum was shifted to the short wavelength region. Because the energy of this transition is conformation-dependent and depends on the molar mass and conjugation length of the macromolecule, the excitation energy is effectively deposited almost in the longest all-trans segments. Thus, the blue shift of the peak suggested that Si-Si bond scission occurred and conjugation length becomes smaller. This was demonstrated by the measurement of the decrease in molar mass during the PMPSi photodegradation.²⁶ Similar results followed also from photoluminescence experiments (cf. Figure 8). It was found that during UV irradiation with 254 nm also photovoltaicization occurs.²⁷ The time dependence of this etching process substantially differed in air and in an Ar atmosphere. In the presence of oxygen an ablation rate of 13 nm min⁻¹ was found for the first 5–10 min exposure, which dropped abruptly to zero (irradiation power density ~ 0.4 mW

cm⁻¹). In an argon atmosphere the etching rate was ca. 0.1 nm min⁻¹ and constant for more than 1 h.

It followed from the energy transfer experiments²⁸ that during the excitation a stretching of the Si bond skeleton could occur. A similar situation has been expected in the polaron formation²⁹ (due to ion-pair dissociation). Positive polaron is characterized by Si-Si bond stretching; at the same time, the Si-Si-Si bond angle decreases in comparison with defect-free chain. In the negative polaron formation the Si-Si bonds are a little stretched, but the Si-Si-Si angles are larger. The stretching of the bonds and the shrinking of the chain conformation leads to the formation of electronic states in the HOMO-LUMO gap. On the other hand, the extension of chain conformation leads to the formation of electronic states outside the gap. These in-gap states follow from the weakened Si bonds (WB) and are expected to be metastable. It could be mentioned that this situation can be realized during weak σ - σ^* excitations when the polysilane chain is not degraded yet but after the radical or ion-pair formation chain deformation occurs. Electronically, the band-edge states are changed by the formation of weakened bonds in the following way.³⁰ The local Si skeleton-bond stretching weakens the $p\sigma$ bonding character of the highest occupied valence-band (HOVB) state, which is formed from the $p\sigma$ bonding state between the skeleton Si 3p_x atomic orbitals, and destabilizes this state. Therefore, the original HOVB state energetically shifts upward, forming a hole-gap state localized around the WB site. Conversely, a reduction in the $sp\sigma^*$ antibonding character (the lowest unoccupied conduction band state, LUCB, is formed from the $sp\sigma^*$ antibonding state between the skeleton Si 2s and 3p_y atomic orbitals) stabilizes the LUCB state energetically, shifting the original LUCB state downward, and an electron-gap state is formed. The appearance of WB's thus interrupts the σ -conjugation of the band-edge states (as it follows from absorption experiments, cf. Figure 2) and creates the tail states. According to quantum chemical calculations²⁸ holes are localized in the position of the WB cutter, whereas the tail-state electrons tend to localize at two Si atoms on this weakened bond.

Because these gap (tail) states for electrons and holes conserve original orbital symmetries of the delocalized band-edge states, optical transitions between them are possible. Thus, these WB's

can act as radiative centers in PMPSi if the excited electron and hole do not separate spatially. This was observed experimentally using photoluminescence (Figure 8). The spectrum measured at 4.2 K with 313 nm excitation consists of a main band with a maximum at 354 nm and a peak at 420 nm which is ascribed to the luminescence from charge-transfer $\sigma\pi^*$ states. Irradiation of the film by “photodegradation light” (366 nm at room temperature for 5 min, curve 2, or 200 min, curve 3, in Figure 8) caused the shift of the main fluorescence peak to the short wavelengths from 354 nm (curve 1, nondegraded sample) to $\lambda \approx 344$ nm (curve 3). This suggested backbone scission and formation of shorter polymer segments or formation of chain disturbances, which limited the effective conjugation length. Generally, the total photoluminescence intensity decreased in the course of photodegradation. However, some increase in photoluminescence (PL) at ca. 520 nm occurred. This “defect” PL emission was effectively observed using the excitation light $\lambda = 365$ nm (see inset in Figure 8) or even with $\lambda = 405$ nm. This photoluminescence intensity increased with the formation of weakened bonds. Thus, we could assume that the additional emissive band is most likely related to photocreated defects in PMPSi. Visually, the luminescence color shifted from blue (for the nondegraded PMPSi sample) to light-green (for sample after “photodegradation”). It should be pointed out that the photoluminescence band at 520 nm manifested good reversibility in the case of moderate excitation of the polymer; it nearly disappeared during the annealing procedure, and the light-green color of the PL at 4.2 K returned to a blue one.

A discussion of energetics leads to the following conclusion: The absorption maximum at 338 nm from the $p\sigma$ (B_{2g}) to $sp\sigma^*$ (B_{3n}) state reflects the HOVB \rightarrow LUCB excitation ($E_g = 3.5$ eV using a $(h\nu\alpha)^2$ vs $h\nu$ plot, where $h\nu$ is the energy of the light quantum and α is the absorption coefficient).³¹ The photoluminescence observed at 510 nm corresponds to the energy 2.4 eV. Thus, the energy difference equals 1.1 eV. If we assume symmetry between the electron and hole tail states, the energy reduction of the band gap can be divided for the contribution of electrons and holes; the trap depth can be in the first approximation estimated as 0.55 eV. An attempt was made to measure the energy of hole traps formed by metastable states directly by TSL.

The result is presented in Figure 9. The TSL curves were measured after excitation with unfiltered light of a high-pressure 500 W mercury lamp for 30 s at 4.2 K. The TSL glow curve of as-prepared sample shows a broad peak with a maximum at $T_m \approx 85$ K. The character of the curve suggests a quasi-continuous trap distribution. The mean activation energy, revealed by the fractional TSL, was determined as $\langle E_m \rangle = 0.19$ eV, and the frequency factor $S \approx 10^{10} \text{ s}^{-1}$.¹² The high-energy wing of the TSL low-temperature peak can well be approximated by a Gaussian distribution of states with the half-width $\sigma = 0.094$ eV. Structural changes induced by UV light in PMPSi at temperature $T \geq 100$ K lead to the modification of TSL spectra: (i) the quantum yield of TSL slightly decreases, and (ii) an additional high-temperature shoulder appears on the main TSL peak in the temperature region of 150–200 K (Figure 9a, curve 1). Drastic changes of the TSL glow curve occurred when the polymer was preliminarily irradiated with UV light at room temperature. In that case, a new TSL peak with a maximum at ca. 190 K appeared (Figure 9a, curve 2); its relative intensity became comparable with the intensity of the main TSL peak. The quantum yield of TSL strongly decreased simultaneously with the appearance of a new TSL peak. The activation energy and frequency factor in the maximum of the new TSL peak were determined as 0.45 eV and $2 \times 10^{10} \text{ s}^{-1}$, respectively. It should be mentioned that photochemical traps, 0.5 eV deep,

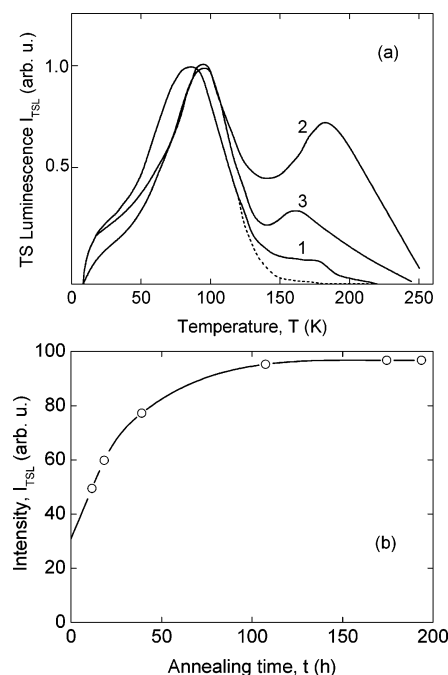


Figure 9. (a) TSL glow curve of as-prepared PMPSi film; excitation with unfiltered light of Hg discharge lamp at 4.2 K (dash curve). Curves 1, 2, and 3 represent normalized TSL spectra after irradiation of the sample with unfiltered light of Hg lamp for 5 min at 150 K (curve 1), at 290 K (curve 2), and after annealing at room temperature for several days (curve 3). (b) Reversibility of the total TSL intensity by annealing at 292 K.

were also detected by thermally stimulated current studies³² and by current post-transient analysis.³³ Annealing of these traps seems to be interesting. The relative intensity of the new peak becomes twice lower after storing the sample in cryostat at room temperature for several days (Figure 9a, curve 3). The quantum yield of the main TSL peak increased concurrently. The effect of annealing is shown in Figure 9b for temperature 292 K. The solid line represents a fit of experimental data by the expression of the type $I \sim (1 - \exp(-t/\tau))$, where I is the total TSL intensity (determined as the area under TSL glow curve), t is the annealing time, and τ is the time constant of the annealing process ($\tau = 32.5$ h at $T = 292$ K). From the temperature dependences activation energy of the annealing process was determined as 0.65 eV.

Both experiments mentioned above, i.e., photo- and thermo-stimulated luminescence, were performed at low temperatures. A question arises if the formation of the metastable states can be induced at room temperature. This was checked by measurements of the optical absorption spectra of PMPSi in a vacuum to avoid the formation of polysiloxane structures and at low photodegradation levels to avoid an irreversible degradation process. The result of the experiment is given in Figure 10. The absorption spectrum of PMPSi film measured in a vacuum at 10^{-4} Pa is given as the top curve in Figure 10a. After photoexcitation with UV light (Hg discharge lamp 200 V, band filter 340 ± 20 nm) for the times given in inset, the spectra showed a similar character as it was presented in Figure 2: the absorbance decreased, and its peak maximum was shifted to short wavelengths. The decrease in the absorbance with “degradation” time is given in inset of Figure 10a. If the sample was kept in a vacuum in the dark, a reversible increase in absorbance was observed. The bottom curve in Figure 10b represents the spectrum immediately after degradation, and the top curve represents the spectrum after annealing at room temperature. The change of the long-wavelength absorbance

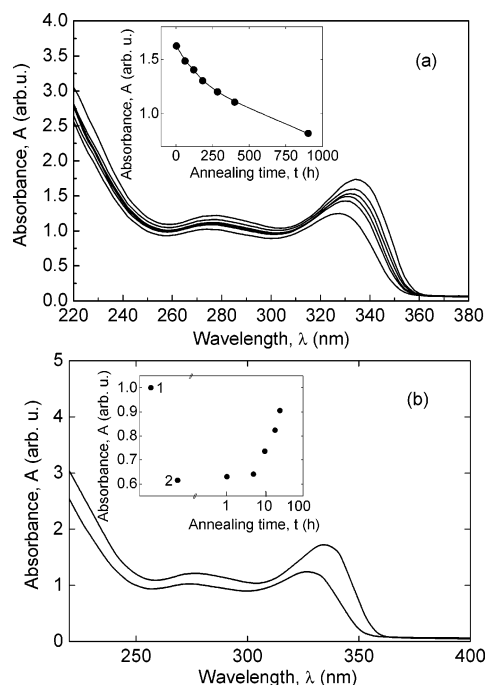


Figure 10. (a) Absorption spectrum of PMPSi film (top curve) and spectra after photodegradation with UV light (Hg discharge lamp 200 W, band filter 340 ± 20 nm) for the times given in the inset. Decrease in absorbance in the inset is related to the decrease in the maximum of the long-wavelength bond. (b) Reversibility in absorption spectrum: bottom curve, spectrum after degradation, top curve, spectrum after annealing at room temperature. The change of the long-wavelength absorbance with annealing time is given in the inset. All measurements were made in a vacuum at 10^{-4} Pa without any air exposure.

with annealing time is given in inset of Figure 10b. Evidently, the reversibility in optical absorption similar to luminescence exists, supporting the idea of the formation of metastable states, which are responsible for trap formation and the decrease in the conjugation length.

Summarizing the effects related to the irradiation of PMPSi films, one can state: In the first step an exciton is formed. An electron from the excited Si–Si bond is transferred from the bonding to antibonding state. Because of σ -conjugation of the Si backbone, the electron can move in the polymer chain (see step V in Figure 7). In this way on-chain electron–hole pairs are formed. The antibonding electron can move back and recombine due to the electrostatic interaction, or jump to another chain to form interchain polar charge transfer (CT) state, or jump to a side group (phenyl, in our case) to form intrachain CT exciton. In both cases dipolar species are formed. They are stabilized by charge carrier traps 0.45–0.50 eV deep which are formed in the vicinity of metastable weakened Si–Si bonds. Simultaneously, material ablation and Si–Si bond scission occur, and radical species and siloxane structures are formed.

As it follows from quantum chemical model calculations of the PMPSi geometry, a dipole is formed with positive polaron on the main chain and localized anion radical on the phenyl group. The angle of the resulting dipole moment with the main chain is ϕ (see Figure 11).

Model of the Liquid-Crystal Alignment. A liquid crystal deposited on an aligned substrate spontaneously develops an equilibrium or easy orientation at the interface characterized by the polar angle θ_0 and the azimuthal angle φ_0 . The polar and azimuthal anchoring energies, $F_p(\theta)$ and $F_a(\varphi)$, specify the energy required to deviate the director from θ_0 and φ_0 , respectively. The relations among these parameters can be expressed in their simplest form using the Rapini–Papoular

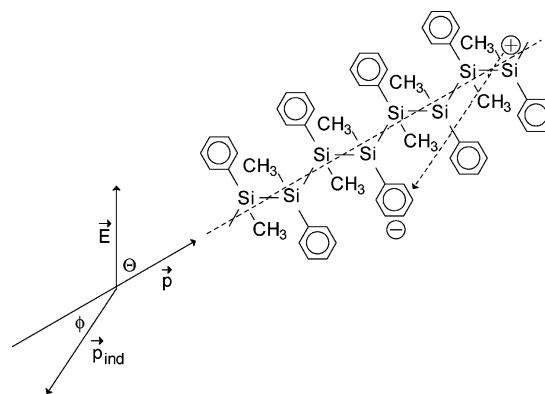


Figure 11. Schematic representation of excitation of the PMPSi chain and formation of an induced dipole of the ion pair. For details, see the text.

approximation: $F_p(\theta) = W_\theta \sin^2(\theta - \theta_0)$; $F_a(\varphi) = W_\varphi \sin^2(\varphi - \varphi_0)$, where W_θ (W_φ) is the polar (azimuthal) part of the anchoring energy. The nature of the LC–polymer surface interaction is complex and includes dispersive (van der Waals), polar, and steric terms. A topological factor can also be involved.

Thus, not only the commonly accepted rule that LC photoalignment is caused by anisotropic intermolecular interaction of LC with the photooriented surface of the polymer film is taken into account.¹ It is known that the presence of dipoles in the oriented polymer film improves the quality of the “in-plane” LC alignment.³⁴ We have shown⁴ that the important step after the excitation of PMPSi is the formation of ion pairs. The cation radicals have usually short lifetimes, say nanoseconds (80 ns in PMPSi powder), if they are formed on one chain as it follows from microwave photoconductivity³⁵ or tens of microseconds^{4,16} (50 μ s in tetrahydrofuran PMPSi solution, 20 μ s in solid film) if they are stabilized by electron transfer from the polysilane backbone to the phenyl group. We have found that the irradiation of PMPSi with UV light results in appearance of traps for positive charges (holes) and generation of excitons and polarons lead to the formation of metastable electron states. This results in the charge carrier trapping and stabilization of ion pairs. The recombination radiation was detected even for several thousands of seconds at 160 K.³⁶ As it follows from the reversibility of the optical absorption mentioned in this paper, the metastable trapping states are active even at room temperature (cf. also ref 37). The long-lifetime ion-pair states were also detected in some other polymers using the collection electric field experiment;³⁸ in poly(*N*-vinylcarbazole) films the ion-pair lifetime was measured as 100 s and in poly(diacetylene) as hundreds of milliseconds.³⁹ One of the important results of this article is the proposal of how the ion pairs could be stabilized: through the chain deformation and metastable states formation due to the existence of excitons and polarons. On irradiation with polarized light one can expect, besides the formation of anisotropic sized bonds and siloxane structures, the formation of an anisotropic distribution of deep traps and oriented ion pairs possessing dipole moments—some sort of nanoelectret network.³⁷ We believe that the anisotropic distribution of such ion pairs could be an important factor for LC alignment.

Irradiation of the PMPSi film with linearly polarized UV light will produce angular dependent photodegradation of the material (see Figure 3). The intensity of the long wavelength band, which arises from the delocalized σ – σ^* electronic transitions, is proportional to the number and length of residual chains. Thus, the higher absorbance will follow from chains perpendicular to the electric field vector of the exciting light. The ordering of residual chains is represented by dichroism calculated at the

wavelength of this transition. The ion pairs are distributed in angles due to the σ -conjugation (cf. Figure 11; note that positive charge is in the main chain and the negative charge is localized on phenyl group). Considering that (i) at the beginning of irradiation the chains, which are oriented parallel to the electric field vector of the exciting light, undergo photodegradation because the probability of the excitation is proportional to $\cos^2 \theta$ (see Figure 11) and (ii) the dipole moment of the ion pair forms the angle ϕ with the chain which was excited, we can conclude that there exists an anisotropic distribution of these dipole moments preferentially oriented parallel to the electric field vector. On further irradiation the chains, which are oriented at angles close to the electric field vector of the exciting light, undergo more and more photodegradation. So, on further irradiation, the anisotropic distribution of the dipole moments of the ion pairs gradually turns to an isotropic distribution. The appearance of the anisotropic distribution of the dipoles is reflected in the azimuthal anchoring energy of the liquid crystal. In the case of the existence of nonzero angle ϕ , the maximum in the azimuthal anchoring energy should precede the maximum of the dichroism, which was observed experimentally. If the angle between the dipole moment of ion pairs and the chains that were excited were equal to zero, the kinetics of the dichroism and azimuthal anchoring energy would correlate.

Conclusion

An exposure to linearly polarized UV light results in the angular-dependent excitation of main-chain segments, which are oriented parallel to the electric field vector of the exciting light. Irradiation of PMPSi films with linearly polarized UV light results in appearance of the photoinduced dichroism. The dichroism is related to the remaining, still intact, Si–Si chain segments perpendicular to the electric field vector of the exciting light. The anisotropic photodegradation induces an anisotropic orientational distribution of the still intact all-trans polysilylene segments and of the photoproducts.

The liquid crystal ZLI-4801-000 deposited on such anisotropic surface become aligned parallel to the electric field vector. This indicates that the remaining all-trans polysilylene segments do not cause the alignment. The alignment is caused by any physical or chemical photoproduct, which are generated preferable parallel to the electric field vector.

Measurements of the photoinduced dichroism in the PMPSi films and the azimuthal anchoring energy of the liquid crystal deposited on these films revealed the absence of correlation in their kinetics. The azimuthal anchoring energy of the liquid crystal reached its maximum just at the beginning of the irradiation when the dichroism was still negligible. On further irradiation the dichroism increased but the azimuthal anchoring energy of liquid crystal dropped to zero. Detailed investigations of photoinduced processes in PMPSi films revealed that excitons and polarons formed during the illumination led to the deformation of the Si–Si skeleton and formation of weakened bonds. Thus, band-gap states are formed in which charge carriers are localized and ion pairs stabilized. Simultaneously, Si–Si bond scission occur and radical species and siloxane structures are formed. The irradiation of PMPSi films with polarized light leads to the formation of a nanoelectret network on the polymer surface due to anisotropic distribution of molecular-sized dipoles (stable charge carrier pairs). This follows from the fact that PMPSi is a highly efficient photoconductor, and a relatively large concentration of charge carriers is generated under illumination. These stable ion pairs are considered to be responsible for the alignment of the liquid crystal deposited on PMPSi surface. On irradiation of a PMPSi film an anisotropic

distribution of the ion pairs is formed. The existence of a nonzero angle between the dipole moment of the ion pairs and the excited chains results in a shift of the maximum of the azimuthal anchoring energy, which precedes the maximum of the dichroism.

Acknowledgment. The financial support by grants Kontakt CZE 03/016 (the project for collaboration between Czech Republic and Germany) and COST 1P04OCD14.30 from the Ministry of Education, Youth and Sports of the Czech Republic, and NATO PST.CLG 978952 is gratefully appreciated.

References and Notes

- (1) O'Neill, M.; Kelly, S. M. *J. Phys. D: Appl. Phys.* **2000**, *33*, R67.
- (2) Miller, R. D.; Michl, J. *Chem. Rev.* **1989**, *89*, 1359.
- (3) Kmínek, I.; Nešpůrek, S.; Brynda, E.; Pfleger, J.; Cimrová, V.; Schnabel, W. *Collect. Czech. Chem. Commun.* **1993**, *58*, 2337.
- (4) Nešpůrek, S.; Eckhardt, A. *Polym. Adv. Technol.* **2001**, *12*, 427.
- (5) Abkowitz, M.; Stolka, M. *J. Inorg. Organomet. Polym.* **1991**, *1*, 487.
- (6) Yuh, H.-J.; Stolka, M. *Philos. Mag. Lett.* **1988**, *58*, 539.
- (7) Nešpůrek, S. *Mater. Sci. Eng.* **1999**, *C 8–9*, 319.
- (8) Miller, R. D.; MacDonald, S. A. *J. Imaging Sci.* **1987**, *31*, 43.
- (9) Dyadyusha, A.; Nešpůrek, S.; Reznikov, Yu.; Kadashchuk, A.; Stumpe, J.; Sapich, B. *Mol. Cryst. Liq. Cryst.* **2001**, *359*, 67.
- (10) Wang, G.; Nešpůrek, S.; Fujii, A.; Yoshino, K. *J. Soc. Electr. Mater. Eng.* **2001**, *10*, 189.
- (11) Sun, R.; Huang, X.; Ma, K.; Jing, H. *SID Proc. IDRC 225* 1994.
- (12) Kadashchuk, A.; Ostapenko, N.; Žaika, V.; Nešpůrek, S. *Chem. Phys.* **1998**, *234*, 285.
- (13) Harrah, L. A.; Zeigler, J. M. *Macromolecules* **1987**, *20*, 610.
- (14) Yaroshchuk, O.; Kadashchuk, A. *Appl. Surf. Sci.* **2000**, *158*, 357.
- (15) Nešpůrek, S.; Dyadyusha, A.; Kadashchuk, A.; Reznikov, Yu.; Stumpe, J. *9th Int. Conference on Unconventional Photoactive Systems; Proc. UPS'99*, **1999**, 132.
- (16) Nešpůrek, S.; Herden, V.; Schnabel, W.; Eckhardt, A. *Czech. J. Phys.* **1998**, *48*, 477.
- (17) Irie, S.; Irie, M. *Macromolecules* **1992**, *25*, 1766.
- (18) Ohsako, Y.; Phillips, J. R. G. C. M.; Zeigler, J. M.; Hochstrasser, R. M. *J. Phys. Chem.* **1989**, *93*, 4408.
- (19) Watanabe, A.; Matsuda, M. *Macromolecules* **1992**, *25*, 484.
- (20) Karatsu, T.; Miller, R. D.; Sooriyakumaran, R.; Michl, J. *J. Am. Chem. Soc.* **1989**, *111*, 1140.
- (21) Meszároš, O.; Schmidt, P.; Pospíšil, J.; Nešpůrek, S. *J. Polym. Sci., Ser. A: Polym. Chem.* **2004**, *42*, 714.
- (22) Pitt, C. G.; Carey, R. N.; Toren, E. C., Jr. *J. Am. Chem. Soc.* **1972**, *94*, 3806.
- (23) Turner, D. W.; Baker, C.; Baker, A. D.; Brundle, C. R. *Molecular Photoelectron Spectroscopy*; Wiley/Interscience: London, 1970.
- (24) Bock, H.; Ensslin, W. *Angew. Chem., Int. Ed. Engl.* **1971**, *10*, 404.
- (25) West, R. *Proc. Symp. Organosilicon*, Pittsburgh, 1971.
- (26) Nešpůrek, S.; Schauer, F.; Kadashchuk, A. *Chem. Monthly* **2001**, *132*, 159.
- (27) Sawodny, M.; Stumpe, J.; Knoll, W. *J. Appl. Phys.* **1991**, *69*, 1927.
- (28) Mintmire, J. W. *Phys. Rev. B* **1989**, *39*, 13350.
- (29) Arkhipov, V. I.; Emelianova, E. V.; Kadashchuk, A.; Blowsky, I.; Nešpůrek, S.; Weiss, D. S.; Bäessler, H. *Phys. Rev. B* **2002**, *65*, 165218.
- (30) Takeda, K.; Shiraishi, K.; Fujiki, M.; Kondo, M.; Margaki, K. *Phys. Rev. B* **1994**, *50*, 5171.
- (31) Navrátil, K.; Šik, J.; Humlíček, J.; Nešpůrek, S. *Opt. Mater.* **1999**, *12*, 105.
- (32) Sanda, P. N.; Samuel, L.; Miller, R. D. *Proc. 3rd Int. SAMPE Electron. Conf.* **1989**, 711.
- (33) Schauer, F.; Handlir, R.; Nešpůrek, S. *Adv. Mater. Opt. Electron.* **1997**, *87*, 61.
- (34) Reznikov, Yu.; Yaroshchuk, O.; Gerus, I.; Homuth, A.; Pelzl, G.; Weissflog, W.; Kim, K. J.; Choi, Y. S.; Kwong, S. B. *Mol. Mater.* **1998**, *9*, 333.
- (35) Nešpůrek, S.; Toman, P.; Sworakowski, J. *Thin Solid Films* **2003**, *438–439*, 268.
- (36) Nešpůrek, S.; Kadashchuk, A.; Skryshevski, Yu.; Fujii, A.; Yoshino, K. *J. Lumin.* **2002**, *99*, 131.
- (37) Naito, H.; Zhang, S.; Okuda, M. *J. Appl. Phys.* **1994**, *76*, 3612.
- (38) Mort, J.; Morgan, M.; Grammatica, S.; Noolandi, J.; Hong, K. M. *Phys. Rev. Lett.* **1982**, *48*, 1411.
- (39) Donovan, K. J.; Elkins, J. W. P.; Wilson, E. G. *Proc. Eur. Conf. Mol. Electron.*, Padua, Italy, 1992.